SPINK1 EXONIC VARIANTS IN CHRONIC PANCREATITIS (PD 120960)

1. Introduction.

Chronic pancreatitis often develops on the basis of genetic susceptibility [1]. Mutations in the PRSS1, CPA1, CTRC, SPINK1, CEL etc. genes coding for pancreatic enzymes are risk factors of pancreatitis [1]. In the past decades, two major pathological pathways were identified in the disease: the trypsin dependent pathway, and the misfolding pathway [2,3]. Under physiological conditions, pancreatic proteases are expressed by pancreatic acinar cells as inactive precursors (zymogens), and secreted into the duodenum where they are activated to fulfill their digestive proteolytic function. Trypsin is the master regulator of zymogen activation, as it converts the trypsin precursor (trypsinogen) to active trypsin, and promotes the activation of other digestive proteases. Its autocatalytic property makes it harmful inside the pancreas, as premature trypsinogen activation may result in auto-digestion of the pancreas and the development of chronic pancreatitis [4]. Therefore, evolutionary protective mechanisms were evolved to protect acinar cells against the intrapancreatic activation of trypsinogen. Chymotrypsin C (CTRC); a minor chymotrypsin isoform, rapidly degrades cationic trypsinogen (PRSS1) in the case of increasing level of active trypsin inside the pancreas [4]. Furthermore, intrapancreatic trypsin will be competitively inhibited by SPINK1, a small protein inhibitor in the pancreas. Gain-of-function mutations in PRSS1 causing increased activation, resistance against degradation or decreased inhibition by SPINK1, are risks for pancreatitis [2]. Consequently, loss of function mutations in CTRC and SPINK1 are also risk factors for the disease. Mutations can cause chronic pancreatitis via the protein misfolding pathway as well [3]. Carboxypeptidase A1 (CPA1), carboxyl ester lipase (CEL) and a small number of PRSS1 mutations are typical examples of this pathway [3,5,6]. These mutations induce improper folding, ER retention of the protein, endoplasmic reticulum stress, and pancreatitis.

Serine protease inhibitor Kazal type 1 (SPINK1) is a trypsin inhibitor secreted by the human pancreas. Its physiological function is to protect the pancreas against premature trypsinogen activation [7]. Genetic studies confirmed that the common SPINK1 mutation p.N34S is enriched 6-folds in cases of chronic pancreatitis, compared to healthy populations [2,8,9]. However, the pathomechanism by which the mutation causes the disease has never been clarified. More than twenty less common mutations with unknown significance were also identified in cases of chronic pancreatitis. We hypothesize that SPINK1 mutations causes pancreatitis due to

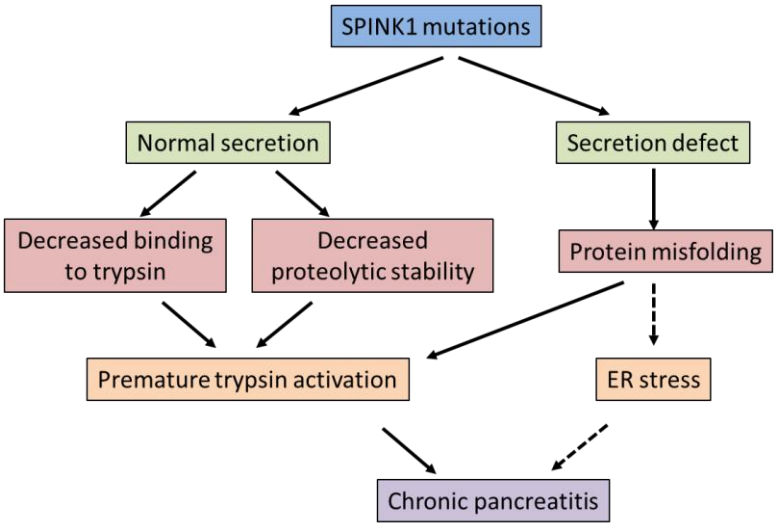

Figure 1. Pathological pathways of SPINK1 missense mutations in chronic pancreatitis.

reduced inhibitor secretion or decreased inhibition of trypsin (Figure 1). Our aim was to functionally characterize SPINK1 mutations found in cases of chronic pancreatitis.

2. Specific aim 1. Functional characterization of SPINK1 mutants.

Human embryonic kidney (HEK) 293T cells are excellent candidates to study the expression of enzymes of the exocrine pancreas. These cells can be readily transfected with plasmid DNA and they secrete SPINK1 wild type and other pancreatic enzymes into the conditioned medium in about 50 nM concentration. In the present project, our goal was to study 22 earlier identified SPINK1 mutants in cases of chronic pancreatitis. The pcDNA3.1(-) expression plasmid carrying the coding region of the human SPINK1 gene and its first intron (minigene 1) was used in the experiments. For mutagenesis, we custom-synthesized mutagenic primer pairs, generated all SPINK1 mutants in the minigene 1 background with overlap extension PCR mutagenesis, and cloned them into the plasmid using the restriction sites XhoI and HindIII. *E. coli* Top10 cells (Life Technologies) were transformed with each plasmid DNA and plated onto LB/agar/ampicillin plates. Colonies were picked and grown for plasmid DNA purification from the bacterial cells using GeneAid plasmid purification kit. The mutations of each SPINK1 clone were verified by performing sequencing PCR reactions with BigDye Terminator v3.1 cycle sequencing kit (Life Technologies), followed by custom sequencing in the Center for Clinical Genomics and Personalized Medicine at University of Debrecen.

2.1. Expression and secretion studies on previously uncharacterized SPINK1 variants.

Six out of the 22 SPINK1 variants identified in cases of chronic pancreatitis (p.L9R, p.K41N, p.I42M, p.P45S, p.V46D, p.R65W) had never been investigated in functional studies.

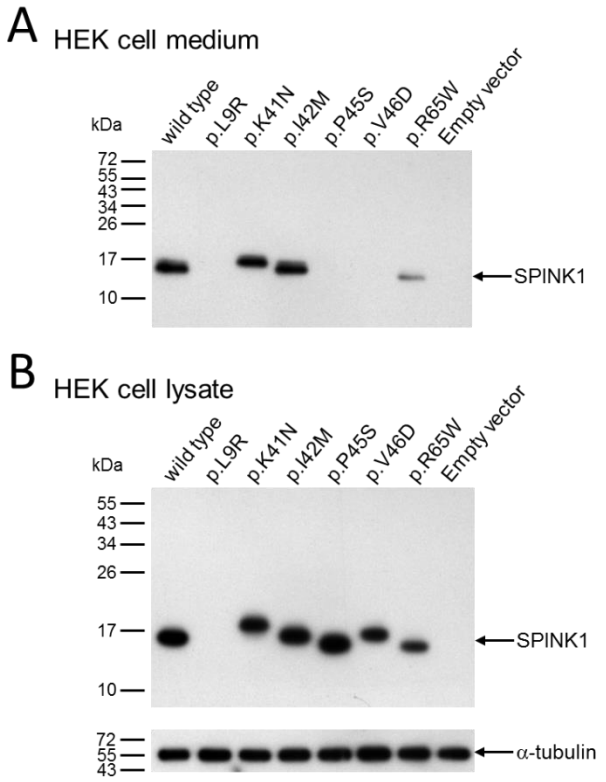

Figure 2. Secretion of previously uncharacterized SPINK1 mutants by HEK 293T cells. Conditioned media (A) and cell lysate (B) of HEK 293T were electrophoresed on 15% SDS-polyacrylamide gels. SPINK1 and alpha-tubulin bands were detected with western blot using penta-His and anti-a-tubulin antibody, respectively.

We transiently transfected HEK 293T cells with plasmid DNA and Lipofectamine 2000 (Thermo Fisher) to study how these mutations affect SPINK1 expression. The cells were cultured in Opti-MEM, and after 48 hour incubation, the media and the cells were harvested. Cells were lysed with a single freeze-thaw cycle using Reporter Lysis 5x buffer (Promega). The secretion of SPINK1 mutants into the conditioned media was tested with SDS-PAGE followed by western blot. SPINK1 protein was detected with HRP conjugated Penta-His antibody (Qiagen), as SPINK1 used in the experiments contained a C-terminal 10His tag (Figure 2). The results indicate that SPINK1 mutants p.K41N and p.I42M were secreted from HEK 293T cells at a comparable level to the wild type. In contrast, SPINK1 mutants p.L9R, p.P45S, p.V46D and p.R65W had severe secretion defect, as most of the mutants could not be detected at all in the conditioned media (Figure 2). To study whether the non-secreted SPINK1 mutants are synthesized normally by the cells, the lysates were subjected to SDS-PAGE and western blot analysis as well. SPINK1 mutant proteins p.K41N, p.I42M, p.P45S, p.V46D and p.R65W were present in the cell lysate at a comparable level to the wild type. Interestingly, SPINK1 signal peptide mutant p.L9R was not detectable inside the cell, probably due to rapid intracellular degradation of the mRNA or the inhibitor. In these experiments, alpha-tubulin served as loading control, detected with mouse anti-tubulin primary antibody (Sigma-Aldrich) and HRP conjugated anti-mouse secondary antibody (Abcam). On the basis of our results and the available literature 6 mutations did not influence SPINK1 secretion, while 16 mutations resulted in reduced secretion out of the investigated 22 mutations (Table 1).

2.2. Functional characterization of SPINK1 variant p.N34S.

The most frequent SPINK1 mutation p.N34S is genetically associated with chronic pancreatitis [9]. However, the mechanism by which the mutation causes the disease remained elusive over the past 20 years. To study the effect of this mutation on trypsin inhibition, we expressed the most abundant human trypsin isoforms (cationic and anionic) using *E. coli* BL21(DE) strain. After purification with ecotin affinity chromatography, trypsin was activated

Table 1. SPINK1 mutations found in cases with chronic pancreatitis.

Exon	Nucleotide change	Amino acid change	Phenotype
1	c.26T>G	p.L9R	non-secreted*
1	c.41T>C	p.L14P	non-secreted
1	c.41T>G	p.L14R	non-secreted
3	c.101A>G	p.N34S	secreted
3	c.110A>G	p.N37S	secreted
3	c.123G>C	p.K41N	secreted*
3	c.126A>G	p.I42M	secreted*
3	c.133C>T	p.P45S	non-secreted*
3	c.137T>A	p.V46D	non-secreted*
3	c.143G>A	p.G48E	non-secreted
3	c.150T>G	p.D50E	non-secreted
3	c.160T>C	p.Y54H	non-secreted
3	c.163C>T	p.P55S	secreted
3	c.190A>G	p.N64D	non-secreted
3	c.193C>T	p.R65W	non-secreted*
3	c.194G>A	p.R65Q	non-secreted
4	c.198A>C	p.K66N	non-secreted
4	c.199C>T	p.R67C	non-secreted
4	c.200G>A	p.R67H	non-secreted
4	c.103A>G	p.Q68R	secreted
4	c.206C>T	p.T69I	non-secreted
4	c.236G>T	p.C79F	non-secreted

Data were obtained from the database

* Results of the present study.

with recombinant human enteropeptidase (R&D Systems). Trypsin concentration was determined with titration against ecotin inhibitor. SPINK1 wild type and mutant p.N34S were expressed on a larger scale by transient transfection of HEK 293T cells. SPINK1 was purified from the conditioned media with a Ni-NTA superflow cartridge (Qiagen). The concentration of SPINK1 was measured with titration against the human trypsins. The binding affinity of SPINK1 to trypsins was determined by measuring equilibrium dissociation constant ($K_{D(eq)}$) values of the enzyme-inhibitor complex (Figure 3A). As an alternative, we also determined the association (k_{on}) and dissociation (k_{off}) rate constants of SPINK1 on the proteases, and K_D was calculated using the equation $K_D=k_{off}/k_{on}$ (Figure 3B). We found that both SPINK1 wild type and mutant p.N34S inhibited cationic trypsin at a comparable level with $K_{D(eq)}$ and K_D values of 1.1-1.4 pM and 1.4-1.6 pM, respectively (Table 2). We also tested the inhibition of anionic trypsin, concluding similar results (K_D values 0.11-0.25 and 0.10-0.40, respectively). Human trypsins are sulfated at Tyr154 located in the S2' substrate binding subsite. We expressed partially and fully sulfated trypsins by HEK 293T cells and purified them with ecotin affinity chromatography. Alternatively, we also purified fully sulfated trypsin isoforms from human pancreatic juice with a MonoQ anion exchanger (GE Healthcare) followed by ecotin affinity chromatography. After activation and concentration determination of trypsins, the $K_{D(eq)}$ and K_D values of SPINK1 and mutant p.N34S were determined. We found that trypsin sulfation decreases SPINK1 binding affinity by an order of magnitude, however the mutation p.N34S did not change the inhibitory function of SPINK1 (Table 2).

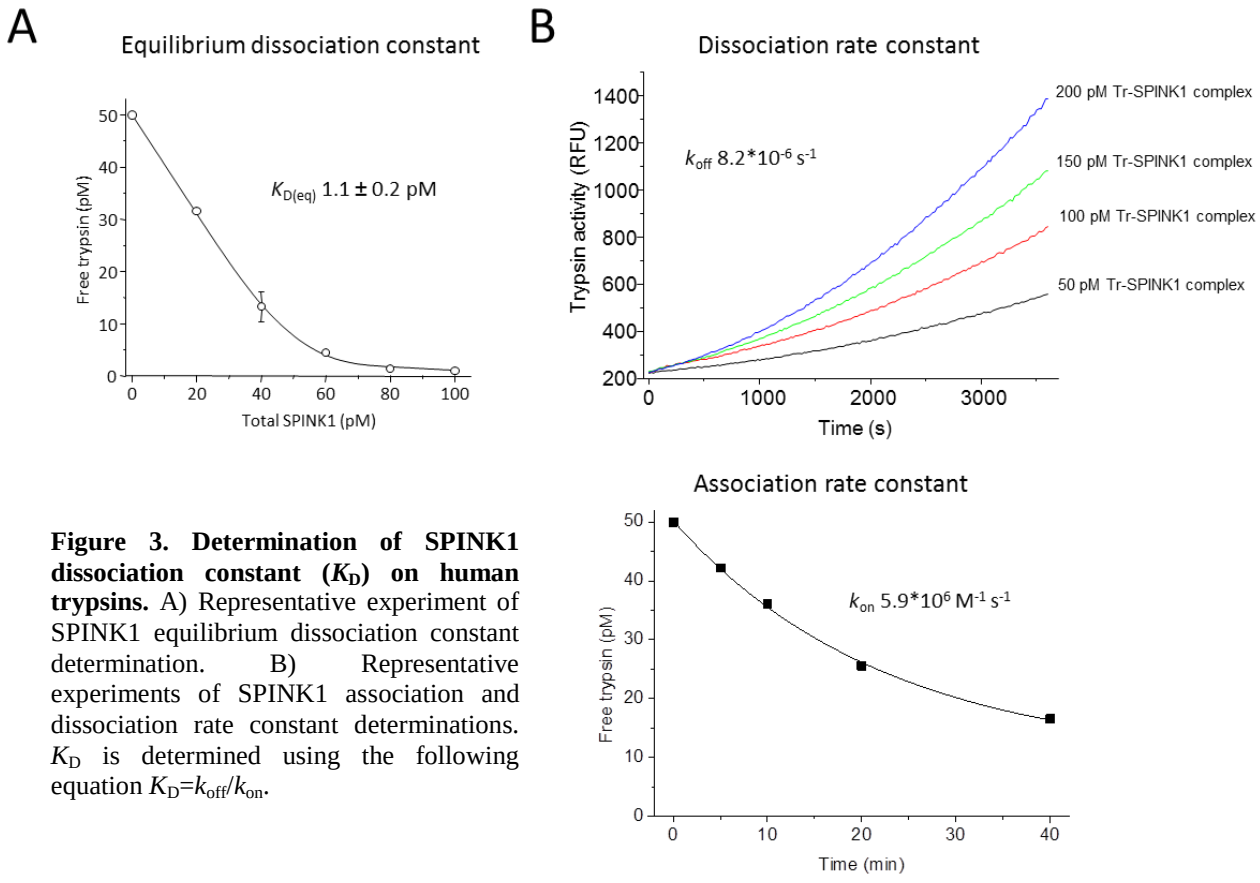

Figure 3. Determination of SPINK1 dissociation constant (K_D) on human trypsins. A) Representative experiment of SPINK1 equilibrium dissociation constant determination. B) Representative experiments of SPINK1 association and dissociation rate constant determinations. K_D is determined using the following equation $K_D=k_{off}/k_{on}$.

Table 2. Dissociation constants (K_D) of SPINK1 wild-type and mutant p.N34S on cationic (Hu1) and anionic (Hu2) trypsins.

SPINK1 wild type

	Tr-Hu1 (*E. coli*)	Tr-Hu1 (HEK)	Tr-Hu1-SO_4 (HEK)	Tr-Hu1-SO_4 (pan. juice)	Tr-Hu2 (*E. coli*)	Tr-Hu2 (HEK)	Tr-Hu2-SO_4 (HEK)	Tr-Hu2-SO_4 (pan. juice)
k_{on} ($M^{-1}s^{-1}$)	5.85 x 10^6	4.97 x 10^6	2.82 x 10^6	2.85 x 10^6	4.57 x 10^6	4.95 x 10^6	1.56 x 10^6	2.25 x 10^6
k_{off} (s^{-1})	8.18 x 10^{-6}	1.72 x 10^{-5}	5.63 x 10^{-5}	5.76 x 10^{-5}	4.97 x 10^{-7}	2.92 x 10^{-6}	1.23 x 10^{-5}	2.18 x 10^{-5}
K_D (pM)	**1.4**	**3.5**	**20.0**	**20.2**	**0.11**	**0.59**	**7.9**	**9.7**
$K_{D(eq)}$ (pM)	**1.1**	**4.4**	**40.2**	**63.2**	**0.25**	**0.53**	**9.0**	**28.6**

SPINK1 p.N34S

	Tr-Hu1 (*E. coli*)	Tr-Hu1 (HEK)	Tr-Hu1-SO_4 (HEK)	Tr-Hu1-SO_4 (pan. juice)	Tr-Hu2 (*E. coli*)	Tr-Hu2 (HEK)	Tr-Hu2-SO_4 (HEK)	Tr-Hu2-SO_4 (pan. juice)
k_{on} ($M^{-1}s^{-1}$)	5.02 x 10^6	4.82 x 10^6	2.76 x 10^6	3.67 x 10^6	4.34 x 10^6	3.09 x 10^6	1.82 x 10^6	2.44 x 10^6
k_{off} (s^{-1})	6.97 x 10^{-6}	1.70 x 10^{-5}	5.33 x 10^{-5}	4.36 x 10^{-5}	4.17 x10^{-7}	2.91 x 10^{-6}	6.20 x 10^{-6}	1.37 x 10^{-5}
K_D (pM)	**1.4**	**3.5**	**19.3**	**11.9**	**0.10**	**0.94**	**3.4**	**5.6**
$K_{D(eq)}$ (pM)	**1.6**	**4.7**	**37.5**	**37.3**	**0.40**	**0.72**	**6.3**	**21.8**

2.3. Functional characterization of rare SPINK1 variants.

We extended our research and functionally characterized rare but readily secreted SPINK1 variants (p.N37S, p.K41N, p.I42M, p.P55S, p.Q68R). Molecular modeling showed that the investigated mutations are located mostly in surface loops, with the exception of mutations p.K41N and p.I42M which are in the inhibitory loop of SPINK1 (Figure 4). We hypothesized that these mutations may cause reduced inhibition of trypsin, therefore we expressed and purified the

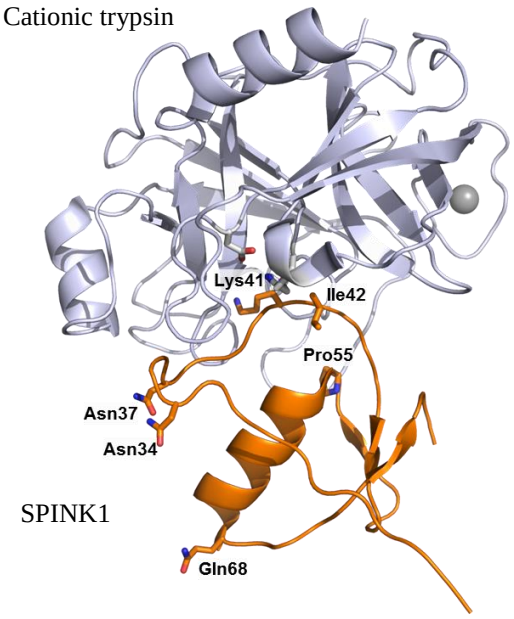

Figure 4. Structural model of SPINK1 in complex with cationic trypsin indicating the mutation sites. The model shows that the mutations are located in loops, including mutations p.K41N and p.I42M which are located in the reactive loop of SPINK1. The image was rendered by fitting the crystallographic coordinates of cationic trypsin in complex with bovine pancreatic trypsin inhibitor (2RA3) and bovine chymotrypsinogen A in complex with SPINK1 (1CGI).

SPINK1 protein variants with nickel affinity chromatography and measured the $K_{D(eq)}$ values against pancreatic trypsin isoforms (Figure 5). Mutations p.I42M and p.P55S, located inside or near the inhibitory loop of SPINK1, increased the $K_{D(eq)}$ value of the inhibitor on cationic trypsin by 3.1-fold and 1.6-fold, respectively. On pancreatic anionic trypsin the same mutations increased SPINK1 $K_{D(eq)}$ values 7.0-fold and 3.3-fold, respectively. The results indicated that SPINK1 variants p.I42M and p.P55S have reduced inhibitory activity on trypsin. More importantly, the inhibitory loop mutation p.K41N completely disrupted the binding of SPINK1 to trypsin isoforms by increasing the $K_{D(eq)}$ value more than four orders of magnitude. The results revealed that the rare SPINK1 mutations p.I42M, p.P55S and p.K41N might be risk factors for chronic pancreatitis, while the pathomechanism by which the common SPINK1 mutation p.N43S causes the disease remained elusive.

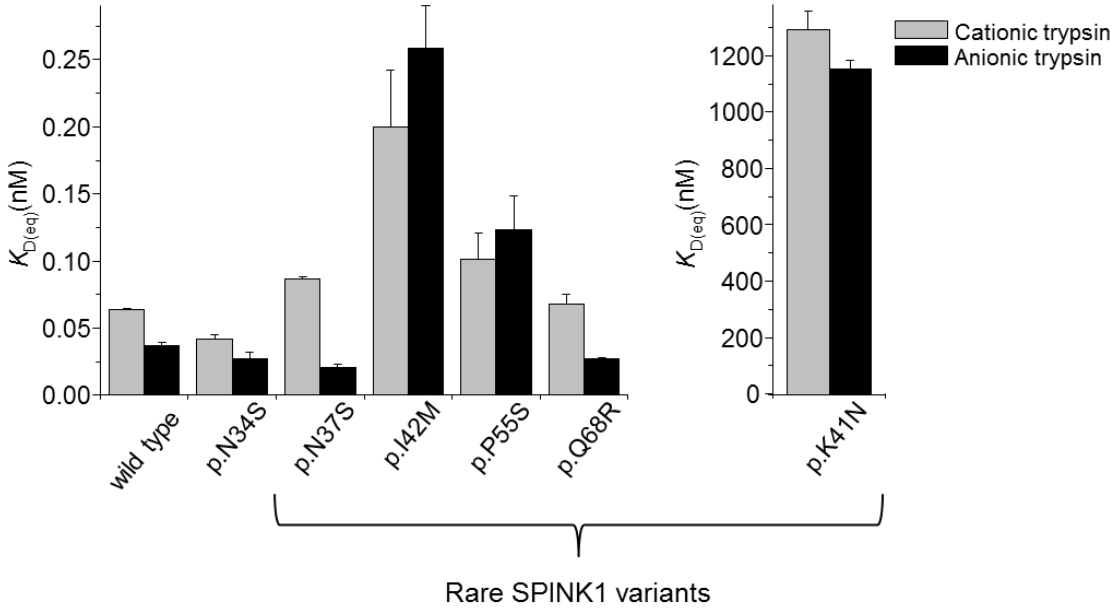

Figure 5. Binding of infrequent SPINK1 mutants to native trypsin isoforms. The equilibrium dissociation constant ($K_{D(eq)}$) of SPINK1 mutants was determined. Note that SPINK1 mutant p.K41N decreased SPINK1 binding affinity by four orders of magnitude, while mutants p.I42M and p.P55S had a less prominent impact.

SPINK1 is a temporary trypsin inhibitor [10,11]. The formation of SPINK1-trypsin complex is reversible, and over time the inhibitory loop of SPINK1 is cleaved by trypsin leading to the inactivation and degradation of the inhibitor. We hypothesized that the reduced binding affinity (increased $K_{D(eq)}$) of SPINK1 mutants p.I42M and p.P55S leads to quicker inhibitor cleavage and inactivation compared to the wild type inhibitor. We mixed 30 nM cationic trypsin with 25 nM SPINK1 wild type or mutant p.I42M. After preincubation for 30 min at 22 ˚C, trypsin activity was followed as a function of time (Figure 6). When trypsin was assayed with SPINK1 wild type, we found that the majority of trypsin initial activity was regained in 24 hours. Trypsin regained its original activity with a slightly higher rate when it was assayed with SPINK1 p.I42M, indicating that the mutant may be a less potent inhibitor of the pancreas and increase the chance for the development of pancreatitis. We also tested the role of mutations p.N34S and p.P55S on SPINK1 degradation by cationic trypsin but these mutations did not increase the rate of inhibitor inactivation (not shown).

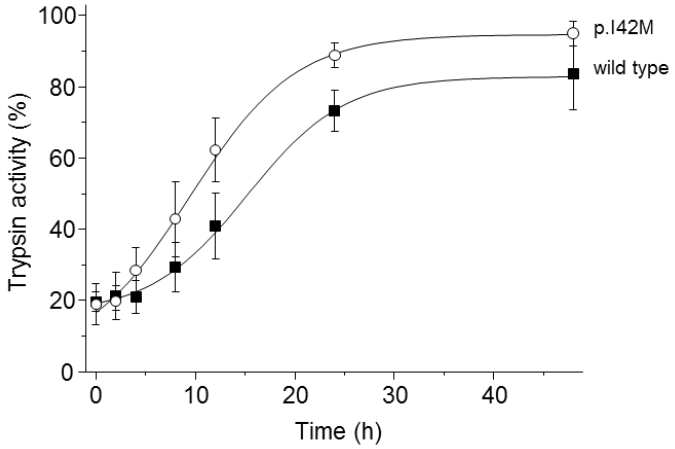

Figure 6. Digestion of SPINK1 wild type and mutant p.I42M by cationic trypsin. SPINK1 at 25 nM was incubated with cationic trypsin at 30 nM. At indicated times aliquotes were withdrawn and trypsin activity was measured at 405 nm using Suc-Ala-Ala-Pro-Lys substrate.

Our functional studies confirmed that SPINK1 mutations p.K41N and p.I42M are possible genetic risk factors of chronic pancreatitis. Although the common SPINK1 mutation p.N34S is genetically associated with pancreatitis, our data strongly suggest that the pathomechanism of this mutant is independent of inhibitory activity.

3. Specific aim 2. Cellular effects of non-secreted SPINK1 mutants

3.1 Role of non-secreted SPINK1 variants in the development of endoplasmic reticulum (ER) stress and cell damage.

In the second part of the project our research mostly focused on the investigation of previously identified non-secreted SPINK1 mutants. Chronic pancreatitis can be developed by mutations in pancreatic proteins causing intracellular protein misfolding, ER stress and cell damage [3]. Previous studies and preliminary experiments identified 16 SPINK1 mutations (p.L9R, p.L14P, p.L14R, p.P45S, p.V46D, p.G48E, p.D50E, p.Y54H, p.N46D, p.R65W, p.R65Q, p.K66N, p.R67C, p.R67H, p.T69I, p.C79F) causing secretion defect in mammalian cells (Table 1). Our aim was to study whether these SPINK1 mutations induce ER stress and cell damage in HEK 293T cells. The cells were cultured on 6-well-plates and transfected with SPINK1 plasmid DNA using Polyethyleneimine (PEI) transfection reagent at 80-90% cell density in DMEM supplemented with 10% FBS and 4 mM Gln. On the next day cells were rinsed with Opti-MEM and further incubated in fresh Opti-MEM. After 48 h incubation the media and the cells were harvested. The secretion defect of SPINK1 mutants was confirmed by SDS-PAGE and western blot analysis of the cell media (not shown), while the cells were lysed and all RNA was isolated. The level of ER stress markers was determined after reverse transcription. Misfolded proteins in the ER may activate IRE1-alpha ribonuclease, which curtails XBP1 mRNA by 26 base pairs, which allows the translation of the XBP1 protein. XBP1 is a transcriptional factor which induces the expression of ER chaperons such as BiP. The level of XBP1 mRNA splicing was detected with PCR and agarose gel electrophoresis (Figure 7). We found that compared to the wild type, SPINK1 mutation p.R67C significantly increased XBP1 mRNA splicing from 23% to 48%, while the other mutations had only minor effects in four independent transfection experiments. Molecular modeling showed that the SPINK1 mutation p.R67C is located in a helical segment of the inhibitor molecule and it may disturb the normal folding of the inhibitor by the formation of incorrect disulfide bonds between cysteine residues (not shown). The level of the chaperon BiP

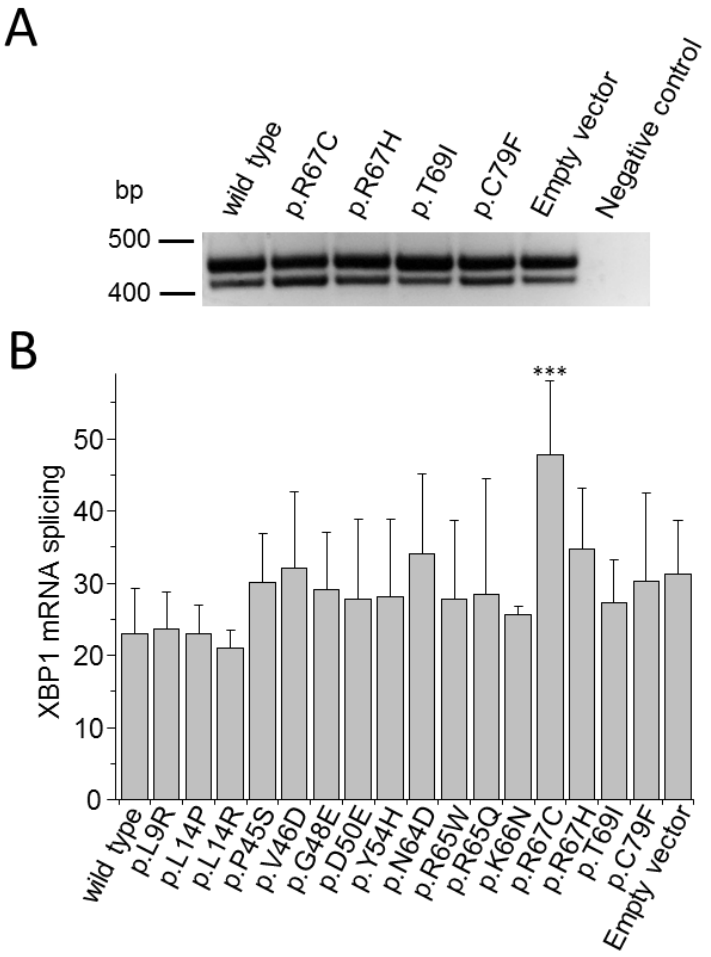

Figure 7. Effect of SPINK1 mutations on the splicing of XBP1 mRNA in HEK 293T. A) Representative agarose gel picture. B) Densitometric analysis of XBP1 mRNA splicing in HEK 293T cells after transfection with SPINK1 wild type and secretion defective mutants.

was also investigated in HEK 293T with real time PCR. The BiP level was normalized to the level of GAPDH in the cDNA samples. In contrast to XBP1, we did not find significant alterations in BiP expression levels in cells transfected with wild type and mutant SPINK1 (not shown).

We also studied the viability of HEK 293AD cells with MTT assay after transient transfection with SPINK1 wild type and mutant p.R67C. We used this cell line instead of the 293T due to its firmer attachment to the plates. As a control, plasmid DNA transfected cells without SPINK1 cDNA served. We found that the expression of SPINK1 wild type did not reduce the viability, while SPINK1 mutant p.R67C decreased the viability by about 20% over the 24 h incubation (Figure 8). Our experiments showed that in HEK cells SPINK1 mutations causing secretion defect did not induce ER stress and cell damage with the exception of mutation p.R67C, which induced substantial XBP1 splicing and decreased cell viability.

3.2. Development of lentiviral vector

Our further aim was to use the AR42J rat pancreatic acinar cell line in SPINK1 secretion experiments, which would give us conclusive results about the pathomechanism of SPINK1 non-secreted mutants. AR42J is more suitable for the investigation of ER stress due to its acinar cell character. However, the delivery of plasmid DNA into this cell type using conventional

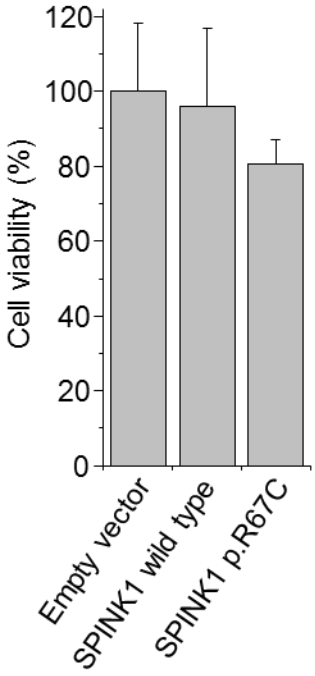

Figure 8. Effect of SPINK1 mutation p.R67C on HEK 293AD viability. The cells were transfected with plasmid DNA carrying SPINK1 wild type and mutant coding sequence. The cells were washed with Opti-MEM and fresh Opti-MEM was added to the wells. After 24 h incubation the cells were subjected to MTT colorimetric assay by the addition of a yellow terazolium salt which turned purple formazan crystals by metabolically active cells in 30 min at 37 ˚C. The crystals were dissolved in DMSO and the absorbance at 544 nm was detected with a plate reader.

transfection reagents is not efficient. In order to deliver SPINK1 DNA into AR42J cells, we developed viral transduction systems. Lentiviral transduction vectors are readily available in the Department of Biochemistry and Molecular Biology at the University of Debrecen. Therefore, we cloned the SPINK1 coding sequence which carries the first intron of SPINK1 gene into the pTy lentiviral vector using the restriction sites SalI and KpnI. By using these restriction sites, the cDNA of GFP protein was removed from the original vector and replaced by the inhibitor. Empty pTy vector was also generated by the removal of the GFP cDNA. To test whether the SPINK1-pTy plasmid is functional, we cultured HEK 293T cells on a 6-well-plate in DMEM supplemented with 10% FBS and transfected the cells at 80-90% confluence with the plasmid DNA and PEI transfection reagent. On the next day, the cells were rinsed with Opti-MEM and fresh Opti-MEM was added to the wells. After 48 h incubation the media were harvested and subjected to trypsin inhibition experiments. 10 nM trypsin was mixed with 0.05 mL conditioned medium containing SPINK1 in 0.1 mL final volume. After 20 min incubation, 0.150 mM Suc-AAPK-pNA substrate was added, and the residual trypsin activity was followed at 405 nm with a plate reader. Medium from cells transfected with empty pTy served as a control. We found full inhibition in assays with media containing SPINK1 protein in contrast to the negative controls where 60 mOD/min trypsin activities were detected. These results indicate that our SPINK1-pTy vector is functional. To produce lentiviral particles carrying our SPINK1 construct we cultured HEK 293T cells in T75 cell culture flasks in DMEM supplemented with 10% FBS and 2 mM Gln. HEK 293T cells were grown to 80% confluence and transfected with the SPINK1-pTy, psPAX2 and pMDG plasmids using polyethyleneimine transfection reagent in DMEM supplemented with 1% FBS and 2 mM Gln. The psPAX2 and pMDG vectors are responsible for the expression of viral structural proteins and packaging of the virus. After 5-6 h incubation the medium was discarded and fresh DMEM containing 10% FBS and 2 mM Gln was added to the flasks. The medium was harvested after 48h and lentiviral particles were isolated with ultracentrifugation at 100000 g for 2 hours. The supernatant was discarded and the pellet was suspended in 0.2 mL PBS. The lentiviral propagation was tested using the Colorimetric reverse

transcriptase assay (Roche). The test reported 150-330 ng/mL reverse transcriptase amount, which corresponds to ~10^9 virions/mL.

3.3. Development of adenoviral vector

Alternatively, we also developed an adenoviral vector carrying SPINK1 DNA to study the effect of SPINK1 mutations on inhibitor secretion in AR42J rat acinar cells. To perform expression studies, SPINK1 coding DNA containing a C-terminal His tag was cloned into the pO6A5 shuttle vector (Sirion Biotech) using the restriction sites NheI and KpnI. The pO6A5-SPINK1 positive clones were verified after transformation of PIR1 competent cells (ThermoFisher Scientific). The expression of SPINK1 was tested after transfection of HEK 293T cells using the protocol described above. E. coli BA5-FRT competent cells (Sirion Biotech) were transformed with the shuttle vector in which the vector was recombined into the endogenous SIR-BAC-Ad5 adenoviral BAC vector. The recombinant BAC vector was isolated from the cells and purified. The BAC DNA was linearized at PacI restriction sites and analyzed on a 0.8% agarose gel. HEK 293AD cells were cultured on a 6-well-plate in DMEM supplemented with 10% FBS and 2 mM Gln and transfected with the linearized BAC DNA and PEI transfection reagent. After three days incubation the cells were harvested, washed in DMEM supplemented with 10% FBS and lysed with freeze-thaw cycles. The isolated adenovirus was amplified in two cycles in HEK 293AD cells using T75 tissue culture flasks. The amplified virions were isolated with freeze-thaw cycles and purified using the AdenoONE Purification Kit (Sirion Biotech). The concentration of functional adenovirus was determined with AdEasy viral titer kit (Agilent). Typical adenovirus titer was about 10^8-10^9 infectious unit per mL.

We compared the efficacy of the lentiviral and adenoviral transduction systems using AR42J rat pancreatic acinar cell line. AR42J was cultured in DMEM supplemented with 20% FBS, 4 mM Gln and 100 nM dexamethasone. After 48 h incubation the cells were rinsed with Opti-MEM and fresh medium was added. The cells were infected with optimal lentivirus (6 ng/mL) or adenovirus (10^6 IU/mL) carrying SPINK1 wild type. After 24 h incubation the conditioned media were harvested and SPINK1 content was determined with titration against cationic trypsin. We found that the adenovirus vector is about 10-fold more effective in SPINK1 gene delivery leading to about 50 nM SPINK1 in 24h, therefore we used adenovirus in our further experiments.

3.4 Cellular effects of SPINK1 p.R67C in acinar cells

AR42J was transfected with adenovirus carrying SPINK1 wild type and p.R67C coding DNA. The level of inhibitor secretion was determined by the analysis of the conditioned media with SDS-PAGE and western blot against HRP conjugated anti-His tag antibody (Figure 9A). We found that the wild type inhibitor was readily secreted from the cells, while the mutant was not detectable in the medium. As secretion defect may induce ER stress in the cells, we studied the level of ER stress markers such as XBP1 mRNA splicing and BiP chaperone expression in the acinar cells (Figure 9B and C). We found that the SPINK1 mutant p.R67C increased XBP1 mRNA splicing by 6-7 fold compared to the effect of the wild type inhibitor. We also tested the expression of BiP chaperone with qPCR and found that the production of SPINK1 mutant p.R67C protein caused a slightly elevated BiP level than the wild type inhibitor in AR42J cells (Figure 9C). We also cultured pancreatic acinar cells obtained from C57BL/6 mice in a 6-well plate following the protocol of Gout et al [12]. After 15 h incubation in a cell culture incubator, the cells were infected with adenovirus vectors carrying the coding DNA of SPINK1 wild type and p.R67C mutant and further incubated for 24 h. The cells and the media were harvested and

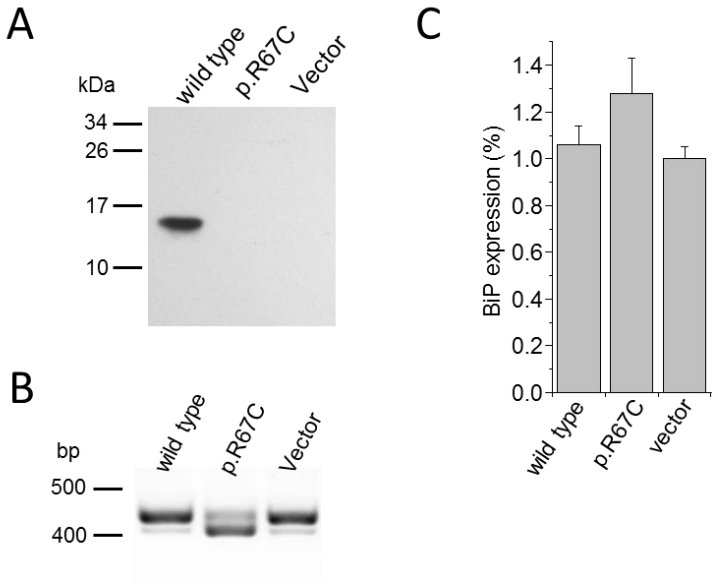

Figure 9. Secretion and cellular effects of SPINK1 wild type and p.R67C in AR42J cells. The cells were transduced with adenovirus carrying SPINK1 wild type and mutant coding sequence. The cells were washed with Opti-MEM and fresh Opti-MEM was added to the wells. After 24 h incubation conditioned media were harvested. A) The secretion of SPINK1 wild type and mutant was followed by the analysis of the conditioned media with SDS-PAGE and western blotting using anti-His antibody. Levels of ER stress markers B) XBP1 mRNA splicing and C) BiP expression were determined with PCR techniques after RNA isolation and reverse transcription.

separated with centrifugation. The cells were lysed with Reporter Lysis 5x buffer (Promega). The expression and secretion of SPINK1 was detected with western blotting using HRP conjugated anti-His antibody (Qiagen). The results indicated no expression of SPINK1 by the mouse primary acinar cells.

3.5. Effect of misfolding phenotype SPINK1 mutation p.R67C in mouse Spink3.

To develop a future mouse model we investigated the effect of several SPINK1 mutations (p.D35S, p.R42N, p.I43M, p.P46S, p.V47D, p.R68C, p.R68H) on the function of the orthologous mouse Spink3. Spink3-10His plasmid was a gift from Dr. Miklós Sahin-Tóth (Boston University). We introduced the mutations into the coding region of Spink3 and cloned the cDNA into pcDNA3.1(-) plasmid using XhoI and HindIII restriction sites. We transfected HEK 293T cells with the plasmid DNA and followed the secretion of Spink3 wild type and mutants with SDS-PAGE and western blot (Figure 10). We found that Spink3 wild type was readily secreted from the cells. Mutations p.D35S, p.R42N, p.I43M and p.R68H did not alter normal Spink3 secretion, while mutations p.P46S, p.V47D and p.R68C completely diminished inhibitor secretion. To investigate the effect of the non-secreted variants on cellular functions, we transfected HEK 293T cells with plasmid DNA carrying Spink3 wild type and p.R68C and isolated RNA from the cells (Figure 10). After reverse transcription, the cDNA was used to detect the level of ER stress marker XBP1 mRNA splicing with PCR and agarose gel electrophoresis. Surprisingly, we found that Spink3 variant p.R68C in HEK cells did not induce XBP1 mRNA splicing and ER stress. To understand the molecular mechanism of this phenomenon more detailed studies are required. We also generated Spink3 single nucleotide deletion mutation p.Y33X causing frame shift and early translation termination. Although the mutation caused secretion defect we could not detect elevated level of ER stress markers in HEK cells (not shown). To test the effect of Spink3 p.R68C mutation on AR42J cells we developed adenovirus vectors carrying Spink3 wild type and mutant cDNAs. We cultured the cells on a 6-well plate as described above and transduced the cells with adenovirus at 10^6 IU/mL. The conditioned media was harvested after 24 h incubation. We found that Spink3 wild type was readily secreted from the cells while the mutant had severe secretion defect (not shown). We lysed the cells and

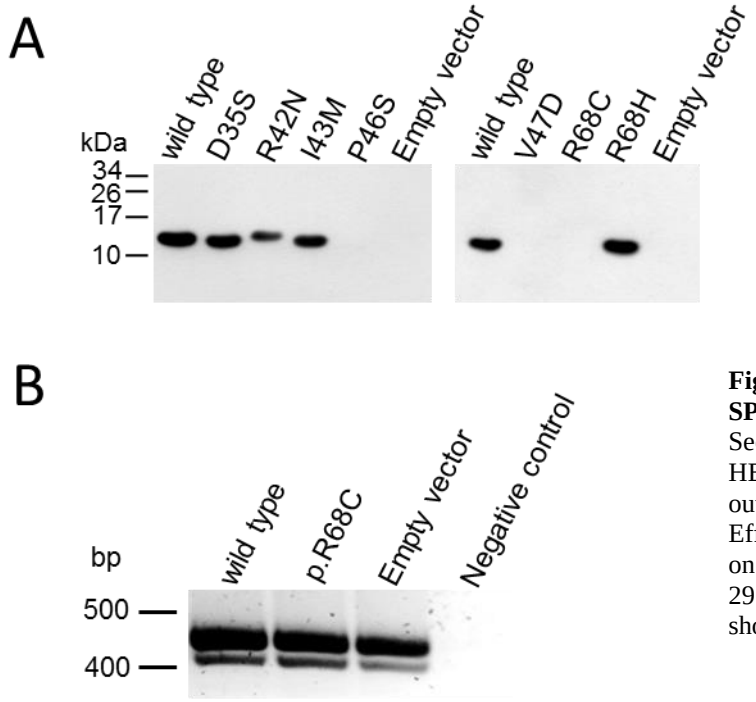

Figure 10. Cellular effects of human SPINK1 mutations in mouse Spink3. A) Secretion of mouse Spink3 variants in HEK 293T cells. Western blot was carried out using anti-pentaHis antibody. B) Effect of mouse Spink3 mutation p.R68C on the splicing of XBP1 mRNA in HEK 293T. Representative gel pictures are shown.

purified RNA. After reverse transcription the level of ER stress marker XBP1 mRNA splicing was monitored with PCR and agarose gel electrophoresis. We found that the level of XBP1 mRNA splicing was comparable in cells expressing the inhibitor wild type and mutant. These observations suggest that mouse model is not a good candidate to investigate the role of Spink3 mutations in pancreatitis induced by protein misfolding.

Our results demonstrated that the majority of non-secreted SPINK1 mutants can cause pancreatitis due to inefficient trypsin inhibition. In addition, SPINK1 p.R67C may induce ER stress in the acinar cells and further increase the chance of disease development or the severity of pancreatitis.

4. References

1. Hasan A, Moscoso DI, Kastrinos F. The Role of Genetics in Pancreatitis. Gastrointest Endosc Clin N Am. 2018;28(4):587–603. doi:10.1016/j.giec.2018.06.001
2. Hegyi E, Sahin-Tóth M. Genetic Risk in Chronic Pancreatitis: The Trypsin-Dependent Pathway. Dig Dis Sci. 2017;62(7):1692–1701. doi:10.1007/s10620-017-4601-3
3. Sahin-Tóth M. Genetic risk in chronic pancreatitis: the misfolding-dependent pathway. Curr Opin Gastroenterol. 2017;33(5):390–395. doi:10.1097/MOG.0000000000000380
4. Szabó A, Sahin-Tóth M. Increased activation of hereditary pancreatitis-associated human cationic trypsinogen mutants in presence of chymotrypsin C. J Biol Chem. 2012;287(24):20701–20710. doi:10.1074/jbc.M112.360065
5. Witt H, Beer S, Rosendahl J, et al. Variants in CPA1 are strongly associated with early onset chronic pancreatitis. Nat Genet. 2013;45(10):1216–1220. doi:10.1038/ng.2730
6. Johansson BB, Fjeld K, El Jellas K, et al. The role of the carboxyl ester lipase (CEL) gene in pancreatic disease. Pancreatology. 2018;18(1):12–19. doi:10.1016/j.pan.2017.12.001

7. Muller N, Sarantitis I, Rouanet M, et al. Natural history of SPINK1 germline mutation related-pancreatitis. EBioMedicine. 2019;48:581–591. doi:10.1016/j.ebiom.2019.09.032
8. Witt H. Genetics of pancreatitis: a guide for clinicians. Dig Dis. 2010;28(6):702–708. doi:10.1159/000324276
9. Witt H, Luck W, Hennies HC, et al. Mutations in the gene encoding the serine protease inhibitor, Kazal type 1 are associated with chronic pancreatitis. Nat Genet. 2000;25(2):213–216. doi:10.1038/76088
10. Schneider SL, Stasiuk L, Laskowski M Sr. Sequence of tryptic cleavages in porcine pancreatic secretory inhibitor II. J Biol Chem. 1973;248(20):7207–7214.
11. Kikuchi N, Nagata K, Shin M, Mitsushima K, Teraoka H, Yoshida N. Site-directed mutagenesis of human pancreatic secretory trypsin inhibitor. J Biochem. 1989;106(6):1059–1063. doi:10.1093/oxfordjournals.jbchem.a122964
12. Gout J, Pommier RM, Vincent DF, et al. Isolation and culture of mouse primary pancreatic acinar cells. J Vis Exp. 2013;(78):50514. Published 2013 Aug 13. doi:10.3791/50514